

Emergence of Many Mini-Circles from a Coffee Suspension with Mechanical Rotation

Hiroshi Ueno ¹, Mayu Shono ¹, Momoko Ogawa ¹, Koichiro Sadakane ^{1,*} and Kenichi Yoshikawa ^{1,2,*} 

¹ Faculty of Life and Medical Sciences, Doshisha University, Tatara, Kyotanabe, Kyoto 610-0394, Japan; uaeneau@dmp1.doshisha.ac.jp (H.U.); smayu1828@gmail.com (M.S.); ctuf1025@mail4.doshisha.ac.jp (M.O.)

² Center for Integrative Medicine and Physics, Institute for Advanced Study, Kyoto University, Kyoto 606-8501, Japan

* Correspondence: ksadakan@mail.doshisha.ac.jp (K.S.); keyoshik@mail.doshisha.ac.jp (K.Y.)

Abstract: Drying of an aqueous suspension containing fine granules leads to the formation of a circular pattern, i.e., the coffee-ring effect. Here, we report the effect of mechanical rotation with drying of an aqueous suspension containing a large amount of granular particles as in the Turkish coffee. It was found that wavy fragmented stripes, or a “waggly pattern”, appear in the early stage of the drying process and a “polka-dot pattern” with many small circles is generated in the late stage. We discuss the mechanism of these patterns in terms of the kinetic effect on micro phase-segregation. We suggest that the waggly pattern is induced through a mechanism similar to spinodal decomposition, whereas polka-dot formation is accompanied by the enhanced segregation of a water-rich phase under mechanical rotation.

Keywords: coffee-ring; micro phase-segregation; transition of drying pattern



Citation: Ueno, H.; Shono, M.; Ogawa, M.; Sadakane, K.; Yoshikawa, K. Emergence of Many Mini-Circles from a Coffee Suspension with Mechanical Rotation. *Physics* **2021**, *3*, 8–16. <https://doi.org/10.3390/physics3010003>

Received: 4 December 2020

Accepted: 14 January 2021

Published: 22 January 2021

Publisher's Note: MDPI stays neutral with regard to jurisdictional claims in published maps and institutional affiliations.



Copyright: © 2021 by the authors. Licensee MDPI, Basel, Switzerland. This article is an open access article distributed under the terms and conditions of the Creative Commons Attribution (CC BY) license (<https://creativecommons.org/licenses/by/4.0/>).

1. Introduction

The formation of a deposition pattern with the evaporation of a liquid containing nonvolatile particles has attracted considerable interest not only from a fundamental scientific aspects perspective [1–3], but also from an engineering point of view with respect to coating and patterning processes [4,5]. As a typical pattern, a so-called coffee-ring is caused by the transportation of solute particles toward a pinned contact line driven by Marangoni effect, or spatial gradient of the surface tension, under a differential evaporation rate over the liquid/air surface [6–11]. In addition to the formation of a ring-like pattern [12], the generation of various kinds of morphologies, such as fractures, cracks, straight lines, spiral and dry parch, have been reported in the drying of droplets containing micro or nanoparticles [13–22]. Smart control of the positioning of nanoparticles by using photo-sensitive surfactant in drying droplets was also reported [23]. It has been shown that particles can be concentrated at the center of a droplet through spot-irradiation of its apex with a heating laser, by dismissing the coffee-ring pattern, which phenomenon was interpreted in terms of the reversal of intra-droplet flow induced by a thermal Marangoni effect [24,25]. A similar manner of particle deposition at the center of a droplet was observed when the solvent was changed from water to octane [26]. To suppress the coffee-ring effect, or the heterogeneous deposition of particles, various methodologies have been proposed, including the application of a surface acoustic wave [27], the imposition of electronic fields [28,29], heating of the solid substrate [30], and the addition of a surfactant [31,32]. In the present study, we performed a drying experiment by adopting an aqueous suspension containing fine coffee powder/granules, i.e., Turkish coffee, which is usually served without filtering and thus contains a relatively large amount of micro-particles. Drying this solution under a horizontal static condition results in the formation of a homogeneous granular layer without the formation of a coffee-ring. Interestingly, characteristic patterns of drying granules,

such as multiple *wavy* segments and several mini-circles, are generated using a rotating dish under a tilting condition.

2. Materials and Methods

Roasted coffee beans were ground with a conical burr coffee grinder (product MSCS-2B, Hario Co. Ltd., Tokyo, Japan). Larger particles were sieved out of the ground powder with a sifter (grid size of 250 μm , Tokyo Screen Co., Ltd., Tokyo, Japan). In Figure 1, the experimental procedure in a schematic manner is shown, together with the photograph of the coffee powder (average diameter of 68 μm , and standard deviation of 23 μm). Aqueous solution was prepared by mixing 900 mg of ground coffee beans with 3 mL of ultrapure water (produced with Milli-Q water purification system, Millipore, Merck). The mixed solution was transferred onto a paper dish, of which the surface laminated with polyethylene terephthalate is hydrophobic and the diameter of the bottom planar part is 140 mm (RS-362, Dixie Japan Ltd., Tokyo, Japan). Then, the solution was mechanically homogenized with a vortex mixer (SI-0286, Scientific Industries Inc., Bohemia, NY, USA). In the present Communication, we report the experimental results under the conditions that the paper dish was fixed to a rotating dish with a tilting angle of $\theta = 45^\circ$ and was rotated at 60 rpm by a direct current motor (mini-motor multi-ratio gearbox (12-speed), item 70190, Tamiya Ltd., Tokyo, Japan). As for the effect of tilting, we found that the coffee solution tends to flow out from the dish when θ is larger than 60° , whereas contrast of the generating pattern becomes relatively unclear when θ is smaller than 30° . Thus, we have carried out the experiment by taking the tilting angle as 45° . Under the condition $\theta = 45^\circ$, when the rotation rate is smaller than 30 rpm, the solution tends to flow downward outside the dish. When the rotation rate is larger than 100 rpm, the generated pattern tends to be inhomogeneous between the inner and outer regions of the dish, because of the relatively large magnitude of the oscillation on the centrifugal force. Based on the results of these preliminary experiments, we report the experimental results at the fixed values of the tilting angle at 45° and rotational rate at 60 rpm, in order to reveal the representable transition of the drying patters between wavy fragmented stripes and many mini-circles.

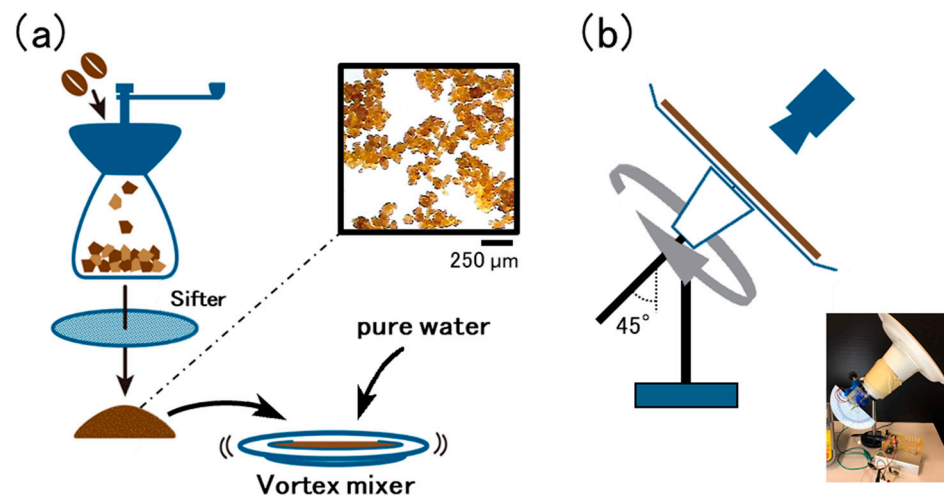


Figure 1. Experimental scheme. (a) Roasted coffee beans were ground with a conical burr grinder. Larger particles were sieved out of the ground powder with a sifter (grid size: 250 μm). The ground coffee was mixed with pure water on a paper dish (diameter of the horizontal circular area: 140 mm), and the solution was spread over the whole dish by vibration with a vortex mixer. (b) Experimental apparatus to rotate the tilted dish with the solution containing the coffee particles. The paper dish with the coffee solution was fixed to a rotating dish with a tilting angle of $\theta = 45^\circ$. The dish was rotated at 60 rpm. During rotation, the whole experimental apparatus was situated inside a control box with constant humidity (60%) and temperature (20 $^\circ\text{C}$).

3. Results and Discussion

Figure 2 shows the drying patterns obtained from the coffee solution, by adopting (a–d) a solution containing coffee powder (see Figure 1a) and (e) filtered solution without powder. All of the pictures were taken for the completely dried states after standing still for 24 h with horizontal positioning. For the experiments shown in (a–d), we used a suspension with the solution of coffee powder on a paper dish, of which the surface is hydrophobic. Figure 2a shows the appearance of a pattern with many wavy shapes, which was obtained by fixing the solution on the tilted plate for 10 s in a stationary manner and then rotating it for 1 min. Hereafter, we call this morphology a “waggly” pattern. Figure 2b shows the drying pattern after 10 s of stationary tilting and then 20 min of plate rotation. The appearance of many mini-circles with a diameter of ~1 mm is observed, which we call “polka-dot” in this article. Here, it is to be noted that the waggly and polka-dot patterns appeared for the same experimental solution with different time-period of the dish rotation. Figure 2c shows a tree-like pattern which was generated under the stationary tilt condition for 1 min without rotation. Figure 2d shows a homogeneous layer of powder obtained by drying the coffee suspension under a horizontal arrangement. For comparison, Figure 2e shows a so-called coffee-ring, which was generated under horizontal drying of a droplet of coffee solution prepared through filtration. In both Figure 2d,e, 0.1 mL of coffee solution was deposited on the paper plate.

As shown in the experimental observations (Figure 2), it has become clear that drying under tilted rotation strongly affects the outcome; a waggly pattern appears first and then a polka-dot pattern develops. Next, we discuss the mechanism of the occurrence of the characteristic patterns. Under dish rotation, the coffee suspension is segregated into grain-rich and water-rich solutions as revealed in Figure 2. It would be expected that the underlying mechanism of the pattern formation observed for the suspension could be interpreted in terms of a kinetic effect in the first-order phase-transition. Thus, we will consider the appearance of the waggly and polka-dot patterns by adopting Cahn–Hilliard-type simple model equations [33–39]:

$$\frac{\partial \eta}{\partial t} = \nabla \left(M_c \nabla \frac{\delta F}{\delta \eta} \right), \quad (1)$$

where the free energy F exhibits two different contributions: bimodality with the order parameter and the interfacial energy. Here, M_c is a parameter of diffusivity and t is time.

$$F = \int \left(L\eta(1 - \eta) + \frac{\alpha}{2} |\nabla \eta|^2 \right) dv, \quad (2)$$

where L , α and dv are interaction parameter, gradient energy coefficient and differential volume, respectively. For simplicity, we chose the bimodal profile of the interaction energy as a function of η , corresponding to the water content in the solution containing coffee grains; $\eta = 1$ corresponds to pure water. We also neglected the contribution from the mixing entropy, since we are considering the segregation of relatively large particles of coffee grains. For the calculation of Equation (2), we tentatively adopted the parameters $L = 6.4 \times 10^3$ J/mol and $\alpha = 3.0 \times 10^{-3}$ Jm²/mol, so as to obtain the pattern with usual spinodal decomposition. We may regard that $\eta = 0, 1$ correspond to the dense coffee grains and the clear solution, respectively. Strictly speaking, our experimental system is non-conservative, because of the evaporation of water to cause the spatial pattern. Thus, the usual Cahn–Hilliard equation does not hold in a strict manner for our experiments, especially for the experimental conditions with relatively large effect of the evaporation. However, the numerical results can still be expected to provide useful insight into the mechanism of pattern formation. Actually, for the initial stage of the drying process when the water content does not decrease so much, the kinetic equation based on Cahn–Hilliard model would represent the essential feature of the segregation. Since the order parameter η is dependent primarily on the relative concentration of the coffee grains, we may need to

consider that the diffusivity M_c is sensitively dependent on η , in addition to the bimodal dependence (the term $\eta(1 - \eta)$),

$$M_c = \left[\frac{D_0}{RT} \eta + \frac{D_1}{RT} (1 - \eta) \right] \eta(1 - \eta), \quad (3)$$

where D_0 and D_1 are the diffusion constants for the states with $\eta = 0$ and 1, respectively. In the following simulation, we used the universal gas constant $R = 8.31$ J/mol. We adopted the apparent diffusion constants $D_0 = 4.0 \times 10^{-10}$ m²/s and $D_1 = 4.0 \times 10^{-8}$ m²/s, by taking into account the effect of the smaller diffusivity of the grain rich solution. We adapted one-order larger value for the apparent diffusivity of water, D_1 , as that of the pure water with stationary standing state [40], by considering the effect owe to the rhythmic change in gravitational field induced by the dish rotation. As for the diffusivity of the grain powder (the diameter is ca. 40 μ m as estimated from the average diameter of 68 μ m, as mentioned in Materials and Methods), it is expected that its diffusion constant is on the order of 10^{-5} – 10^{-6} compared to that of water for the usual Brownian motion under thermal equilibrium, as estimated from the Stokes–Einstein relationship. In addition, with the decrease of the water content, the diffusion of the coffee grain should become much lower. Thus, it is noted that the adapted value for D_1 is rather large compared to the intrinsic diffusivity under the fluctuation-dispersion relationship near thermal equilibrium. In other words, we perform the numerical modeling with the consideration of the effect induced by the external agitation, i.e., the periodic change of the gravitational field accompanied by the rotation of the tilted dish. Through such simple assumptions, we performed a numerical simulation using a two-dimensional system to shed light on the essential mechanism on the time-development of the generated pattern. It may be possible to include the effect of the periodic acceleration during dish rotation by tuning the effective temperature in the simulation. However, in the present study, for simplicity we used room temperature, $T = 293$ K. We carried out the numerical simulation by modifying the source code of Python available from the open access version [41], provided by the “Yamanaka Laboratory” at Tokyo University of Agriculture and Technology, Japan. The grid spacing in the computation is taken as 1.0×10^{-3} m. The time width and step number are 0.01 s and 13,000, respectively; corresponding to a time-period of 130 s.

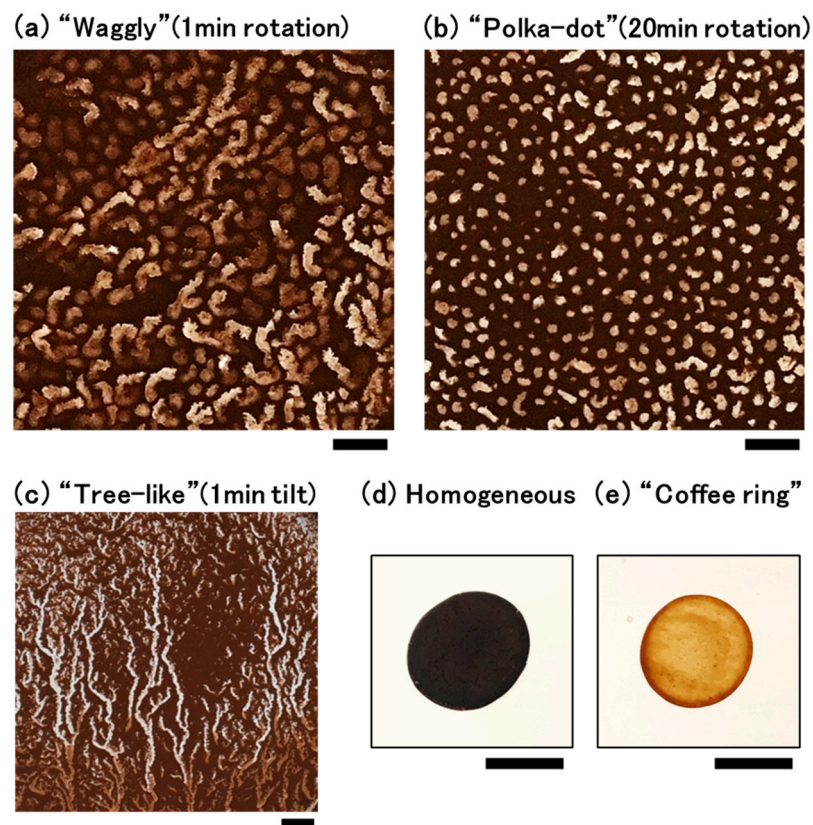


Figure 2. Generation of various characteristic patterns from a drying solution containing coffee powder under different conditions. The scale bars are 10 mm. (a) A waggly pattern with many wavy shapes formed when the paper dish was tilted while stationary for 10 s and then rotated for 1 min at a fixed angle of 45° (see Figure 1b). After the rotation, the dish was stood still horizontally for 24 h. The light brown and dark brown parts indicate water-rich and powder-rich regions, respectively. (b) Polka-dot pattern with many mini-circles generated from the coffee solution, with tilting without rotation for 10 s and then rotation for 20 min. After the rotation, the dish was stood still horizontally for 24 h. (c) Tree-like pattern caused by the downward flow of coffee solution when the plate was tilted at a fixed angle of 45° for 1 min without rotation, the dish was stood still horizontally for 24 h. (d) Homogeneous pattern formed by drying the coffee solution containing the powder, i.e., essentially the same solution as in (a–c). (e) Usual so-called coffee-ring formed by drying the filtered coffee solution with almost no grained powder.

Figure 3 exemplifies the segregation pattern generated after 130 s from the start of the segregation in the simulation. Figure 3a shows the appearance of wavy short-fragmented stripes, where the coloring of the segregation pattern is carried out with a threshold value of $\eta = 0.53$. This wavy pattern is familiar for phase segregation with spinodal decomposition [42] and apparently is similar to the waggly pattern observed in the early state (1 min rotation) of the drying process with vessel rotation as in Figure 2a. In contrast, Figure 3b shows the appearance of many mini-circles when the threshold is $\eta = 0.56$, corresponding to the polka-dot pattern observed in the late stage with rotation as in Figure 2b. Here, note that the apparent patterns change markedly depending on the threshold value for the same stage of the phase segregation kinetics. Figure 3c shows the spatial profile of the order parameter for the same region as in Figure 3a,b, revealing the existence of multiple domains with a larger η value along a wavy stripe. The appearance of multiple spots implies the occurrence of mini water-rich spots and such water-rich regions would prefer the formation of round shaped domain owe to the effect of surface tension. Thus, it is expected that such water-rich mini-domains tend to develop circular aqueous droplets during the longer drying process with rotation under tilting. The rate of water

evaporation is expected to be faster in the grain-rich region (corresponding to the domain with smaller parameter η) compared to that from the relatively smooth surface of the mini water-rich region, which may induce the formation of mini water droplets with circular shapes by causing the polka-dot pattern.

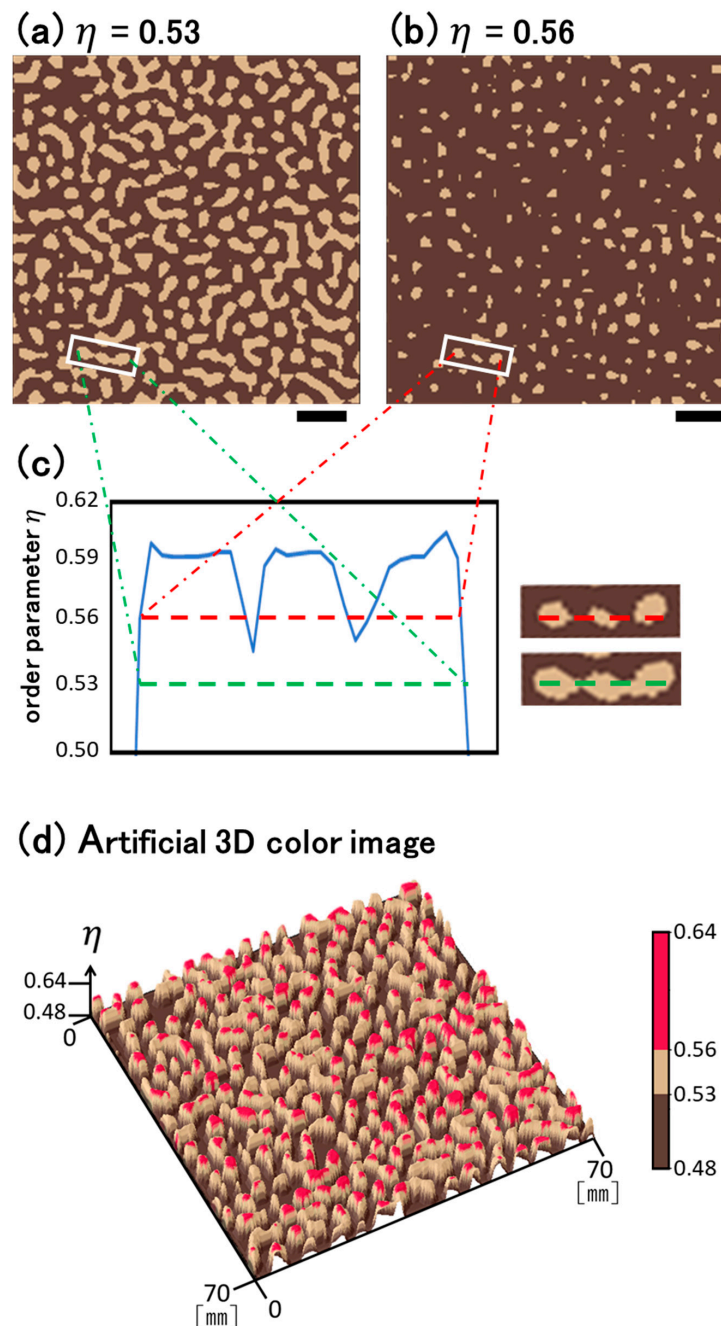


Figure 3. Segregation pattern obtained from numerical simulation for phase-segregation with the simple model equations (Equations (1)–(3)). The scale bars are 10 mm. (a,b): Spatial patterns with different threshold values of the parameter, $\eta = 0.53$ and 0.56 , respectively, both of which correspond to the pattern generated after 130 s from the start of segregation. The bright parts in (b) show the region that is more water-rich than that in (a). (c): Order parameter along a section as indicated by a green bar in (a) and a red bar in (b), which are chosen from the spatial patterns in (a,b). (d): Artificial 3D color image on the same numerical simulation as in (a,b), revealing the existence of mini water-rich spots on the upper part (larger η value) of the waggly pattern.

4. Conclusions

We have reported the formation of waggly and polka-dot patterns for a drying solution containing fine coffee granules under tilted rotation. The results showed that mm-sized phase-segregation between the powder-rich and water-rich phases occurs for the drying solution with dish-rotation, whereas a homogeneous drying layer is generated without rotation. In relation to our observation, the appearance of various unique patterns from a coffee solution with a large amount of grain powder is known as a “fortune telling” pattern with Turkish coffee [43]. Inspired by such interesting pattern formation, we have performed the present study by introducing the effect of mechanical rotation of the plate. The appearance of the polka-dot pattern implies the realization of a uniform pattern with many mini-circles. It is noted that the time-development from waggly onto polka-dot pattern implies a kind of reverse process of coarse-graining. On the other hand, it is well known that coarsening or Ostwald ripening is the usual scenario in spinodal decomposition. Recently, it has been suggested that assemblies of self-propelled particles can cause reverse Ostwald ripening, i.e., reverse process of coarsening [44]. As similar phenomenon, the formation of spherical domains through the kinetics of spinodal decomposition was observed for a rubber-modified epoxy resin accompanied by a chemical reaction [45–48]. It is also noted that, from theoretical considerations, self-propelled particles are expected to undergo phase-separation [49–51], suggesting the occurrence of reverse process of coarsening during the development of phases separation. Thus, it is expected that the occurrence of the reverse-coarsening is generated under the far-equilibrium conditions through the violation of the fluctuation-dissipation relationship, or caused by the external mechanical agitation. In our experiment, the periodic change of the gravitational field should cause fluctuating translational motion of the segregating domains and such forcing effect may concern with the underlying mechanism on the specific phase-segregation of self-propelled particles under the violation of the fluctuation-dissipation relationship. The results of the present study as in Figure 2 suggest that the formation of many mini-circular pattern from waggly pattern, or reverse Ostwald ripening, can be generated for passive particles under external agitation of the mechanical dish rotation with a tilted state. Here, it is to be noted that, for the transition of the patterns, surface tension should play an important role in the formation of the circular domain as in the Polka-dot pattern through the decrease of the droplet surface area in the water-rich domains. In our 2D model simulation, we have not adapted these important effects in an apparent manner. It is highly expected that our results will stimulate experimental studies to examine the possible appearance of unique drying-induced patterns for solutions under various types of external mechanical agitation and also theoretical studies to clarify the detailed mechanism of the time-development from waggly pattern onto polka-dot pattern.

Author Contributions: Conceptualization and methodology, H.U.; investigation, H.U., M.S., M.O.; writing—original draft preparation, H.U., M.S., M.O.; writing—review and editing, K.S., K.Y.; Supervision, K.Y. All authors have read and agreed to the published version of the manuscript.

Funding: This work was partially supported by JSPS KAKENHI Grant Number JP20H01877 awarded to K.Y.

Data Availability Statement: Data available in a publicly accessible repository.

Acknowledgments: We are grateful to Mana Shimobayashi for her technical support with the experimental observation. H.U. acknowledges the support by Yoshida Scholarship Foundation. We thank S. Hagino for the technical advice concerning Turkish coffee.

Conflicts of Interest: The authors declare no conflict of interest.

References

1. Deegan, R.D.; Bakajin, O.; Dupont, T.F.; Huber, G.; Nagel, S.R. Capillary Flow as the Cause of Ring Stains from Dried Liquid Drops. *Nature* **1997**, *5*, 736. [[CrossRef](#)]
2. Carrithers, A.D.; Brown, M.J.; Rashed, M.Z.; Islam, S.; Velev, O.D.; Williams, S.J. Multiscale Self-Assembly of Distinctive Weblike Structures from Evaporated Drops of Dilute American Whiskeys. *ACS Nano* **2020**, *14*, 5417–5425. [[CrossRef](#)] [[PubMed](#)]
3. Thiele, U.; Todorova, D.V.; Lopez, H. Gradient Dynamics Description for Films of Mixtures and Suspensions: Dewetting Triggered by Coupled Film Height and Concentration Fluctuations. *Phys. Rev. Lett.* **2013**, *111*, 117801. [[CrossRef](#)] [[PubMed](#)]
4. Park, J.; Moon, J. Control of Colloidal Particle Deposit Patterns within Picoliter Droplets Ejected by Ink-Jet Printing. *Langmuir* **2006**, *22*, 3506–3513. [[CrossRef](#)]
5. Kuang, M.; Wang, L.; Song, Y. Controllable Printing Droplets for High-Resolution Patterns. *Adv. Mater.* **2014**, *26*, 6950–6958. [[CrossRef](#)]
6. Deegan, R.D.; Bakajin, O.; Dupont, T.F.; Huber, G.; Nagel, S.R.; Witten, T.A. Contact Line Deposits in an Evaporating Drop. *Phys. Rev. E* **2000**, *62*, 756–765. [[CrossRef](#)]
7. Hampton, M.A.; Nguyen, T.A.H.; Nguyen, A.V.; Xu, Z.P.; Huang, L.; Rudolph, V. Influence of Surface Orientation on the Organization of Nanoparticles in Drying Nanofluid Droplets. *J. Colloid Interface Sci.* **2012**, *377*, 456–462. [[CrossRef](#)] [[PubMed](#)]
8. Weon, B.M.; Je, J.H. Fingering inside the Coffee Ring. *Phys. Rev. E* **2013**, *87*, 013003. [[CrossRef](#)]
9. Li, Y.; Diddens, C.; Segers, T.; Wijshoff, H.; Versluis, M.; Lohse, D. Evaporating Droplets on Oil-Wetted Surfaces: Suppression of the Coffee-Stain Effect. *Proc. Natl. Acad. Sci. USA* **2020**, *117*, 16756–16763. [[CrossRef](#)]
10. Parsa, M.; Harmand, S.; Sefiane, K. Mechanisms of Pattern Formation from Dried Sessile Drops. *Adv. Colloid Interface Sci.* **2018**, *254*, 22–47. [[CrossRef](#)]
11. Still, T.; Yunker, P.J.; Yodh, A.G. Surfactant-Induced Marangoni Eddies Alter the Coffee-Rings of Evaporating Colloidal Drops. *Langmuir* **2012**, *28*, 4984–4988. [[CrossRef](#)] [[PubMed](#)]
12. Hu, G.; Yang, L.; Yang, Z.; Wang, Y.; Jin, X.; Dai, J.; Wu, Q.; Liu, S.; Zhu, X.; Wang, X.; et al. A General Ink Formulation of 2D Crystals for Wafer-Scale Inkjet Printing. *Sci. Adv.* **2020**, *6*, eaba5029. [[CrossRef](#)]
13. Parris, F.; Allain, C. Drying of Colloidal Suspension Droplets: Experimental Study and Profile Renormalization. *Langmuir* **1997**, *13*, 3598–3602. [[CrossRef](#)]
14. Sugiyama, Y.; Larsen, R.J.; Kim, J.-W.; Weitz, D.A. Buckling and Crumpling of Drying Droplets of Colloid–Polymer Suspensions. *Langmuir* **2006**, *22*, 6024–6030. [[CrossRef](#)] [[PubMed](#)]
15. Sen, D.; Melo, J.S.; Bahadur, J.; Mazumder, S.; Bhattacharya, S.; Ghosh, G.; Dutta, D.; D’Souza, S.F. Buckling-Driven Morphological Transformation of Droplets of a Mixed Colloidal Suspension during Evaporation-Induced Self-Assembly by Spray Drying. *Euro. Phys. J. E* **2010**, *31*, 393–402. [[CrossRef](#)]
16. Bück, A.; Peglow, M.; Naumann, M.; Tsotsas, E. Population Balance Model for Drying of Droplets Containing Aggregating Nanoparticles. *AIChE J.* **2012**, *58*, 3318–3328. [[CrossRef](#)]
17. Goehring, L.; Clegg, W.J.; Routh, A.F. Plasticity and Fracture in Drying Colloidal Films. *Phys. Rev. Lett.* **2013**, *110*, 024301. [[CrossRef](#)]
18. Li, W.; Lan, D.; Wang, Y. Dewetting-Mediated Pattern Formation inside the Coffee Ring. *Phys. Rev. E* **2017**, *95*, 042607. [[CrossRef](#)]
19. Winkler, A.; Virnau, P.; Binder, K.; Winkler, R.G.; Gompper, G. Hydrodynamic Mechanisms of Spinodal Decomposition in Confined Colloid-Polymer Mixtures: A Multiparticle Collision Dynamics Study. *J. Chem. Phys.* **2013**, *138*, 054901. [[CrossRef](#)]
20. Varanakkottu, S.N.; Anyfantakis, M.; Morel, M.; Rudiuk, S.; Baigl, D. Light-Directed Particle Patterning by Evaporative Optical Marangoni Assembly. *Nano Lett.* **2016**, *16*, 644–650. [[CrossRef](#)]
21. Joksimovic, R.; Watanabe, S.; Riemer, S.; Gradzielski, M.; Yoshikawa, K. Self-Organized Patterning through the Dynamic Segregation of DNA and Silica Nanoparticles. *Sci. Rep.* **2014**, *4*, 3660. [[CrossRef](#)] [[PubMed](#)]
22. Mae, K.; Toyama, H.; Nawa-Okita, E.; Yamamoto, D.; Chen, Y.-J.; Yoshikawa, K.; Toshimitsu, F.; Nakashima, N.; Matsuda, K.; Shioi, A. Self-Organized Micro-Spiral of Single-Walled Carbon Nanotubes. *Sci. Rep.* **2017**, *7*, 5267. [[CrossRef](#)] [[PubMed](#)]
23. Anyfantakis, M.; Varanakkottu, S.N.; Rudiuk, S.; Morel, M.; Baigl, D. Evaporative Optical Marangoni Assembly: Tailoring the Three-Dimensional Morphology of Individual Deposits of Nanoparticles from Sessile Drops. *ACS Appl. Mater. Interfaces* **2017**, *9*, 37435–37445. [[CrossRef](#)] [[PubMed](#)]
24. Yen, T.M.; Fu, X.; Wei, T.; Nayak, R.U.; Shi, Y.; Lo, Y.-H. Reversing Coffee-Ring Effect by Laser-Induced Differential Evaporation. *Sci. Rep.* **2018**, *8*, 3157. [[CrossRef](#)] [[PubMed](#)]
25. Mouhamad, Y. Dynamics and Phase Separation during Spin Casting of Polymer Films. Ph.D. Thesis, University of Sheffield, Sheffield, UK, 2014.
26. Hu, H.; Larson, R.G. Marangoni Effect Reverses Coffee-Ring Depositions. *J. Phys. Chem. B* **2006**, *110*, 7090–7094. [[CrossRef](#)]
27. Mampallil, D.; Reboud, J.; Wilson, R.; Wylie, D.; Klug, D.R.; Cooper, J.M. Acoustic Suppression of the Coffee-Ring Effect. *Soft Matter* **2015**, *11*, 7207–7213. [[CrossRef](#)]
28. Kim, S.J.; Kang, K.H.; Lee, J.-G.; Kang, I.S.; Yoon, B.J. Control of Particle-Deposition Pattern in a Sessile Droplet by Using Radial Electroosmotic Flow. *Anal. Chem.* **2006**, *78*, 5192–5197. [[CrossRef](#)]
29. Wray, A.W.; Papageorgiou, D.T.; Craster, R.V.; Sefiane, K.; Matar, O.K. Electrostatic Suppression of the “Coffee Stain Effect”. *Langmuir* **2014**, *30*, 5849–5858. [[CrossRef](#)]
30. Li, Y.; Lv, C.; Li, Z.; Quéré, D.; Zheng, Q. From Coffee Rings to Coffee Eyes. *Soft Matter* **2015**, *11*, 4669–4673. [[CrossRef](#)]
31. Anyfantakis, M.; Geng, Z.; Morel, M.; Rudiuk, S.; Baigl, D. Modulation of the Coffee-Ring Effect in Particle/Surfactant Mixtures: The Importance of Particle–Interface Interactions. *Langmuir* **2015**, *31*, 4113–4120. [[CrossRef](#)]

32. Chao, Y.; Hung, L.T.; Feng, J.; Yuan, H.; Pan, Y.; Guo, W.; Zhang, Y.; Shum, H.C. Flower-like Droplets Obtained by Self-Emulsification of a Phase-Separating (SEPS) Aqueous Film. *Soft Matter* **2020**, *16*, 6050–6055. [[CrossRef](#)] [[PubMed](#)]
33. Cahn, J.W.; Hilliard, J.E. Free Energy of a Nonuniform System. I. Interfacial Free Energy. *J. Chem. Phys.* **1958**, *28*, 258–267. [[CrossRef](#)]
34. Yamanaka, A.; Aoki, T.; Ogawa, S.; Takaki, T. GPU-Accelerated Phase-Field Simulation of Dendritic Solidification in a Binary Alloy. *J. Cryst. Growth* **2011**, *318*, 40–45. [[CrossRef](#)]
35. Lee, D.; Huh, J.-Y.; Jeong, D.; Shin, J.; Yun, A.; Kim, J. Physical, Mathematical, and Numerical Derivations of the Cahn–Hilliard Equation. *Comput. Mat. Sci.* **2014**, *81*, 216–225. [[CrossRef](#)]
36. Liu, J.; Dedè, L.; Evans, J.A.; Borden, M.J.; Hughes, T.J.R. Isogeometric Analysis of the Advective Cahn–Hilliard Equation: Spinodal Decomposition under Shear Flow. *J. Comp. Phys.* **2013**, *242*, 321–350. [[CrossRef](#)]
37. Alizadeh Pahlavan, A.; Cueto-Felgueroso, L.; Hosoi, A.E.; McKinley, G.H.; Juanes, R. Thin Films in Partial Wetting: Stability, Dewetting and Coarsening. *J. Fluid Mech.* **2018**, *845*, 642–681. [[CrossRef](#)]
38. Li, Y.; Pang, Y.; Liu, W.; Wu, X.; Hou, Z. Effect of Diffusivity on the Pseudospinodal Decomposition of the Γ' Phase in a Ni–Al Alloy. *J. Phase Equilib. Diffus.* **2016**, *37*, 261–268. [[CrossRef](#)]
39. Tran Duc, V.-N.; Chan, P.K. Using the Cahn–Hilliard Theory in Metastable Binary Solutions. *ChemEngineering* **2019**, *3*, 75. [[CrossRef](#)]
40. Holz, M.; Heil, S.R.; Sacco, A. Temperature-Dependent Self-Diffusion Coefficients of Water and Six Selected Molecular Liquids for Calibration in Accurate 1H NMR PFG Measurements. *Phys. Chem. Chem. Phys.* **2000**, *2*, 4740–4742. [[CrossRef](#)]
41. Two-Dimensional Phase-Field Model for Conserved Order Parameter (Cahn–Hilliard Equation). Available online: <http://web.tuat.ac.jp/~yamanaka/pcoms2019/Cahn-Hilliard-2d.html> (accessed on 31 October 2020).
42. Elder, K.; Rogers, T.; Desai, R. Early Stages of Spinodal Decomposition for the Cahn–Hilliard–Cook Model of Phase Separation. *Phys. Rev. B* **1988**, *38*, 4725–4739. [[CrossRef](#)]
43. Nicolaou, L. *The Art of Coffee Cup Reading*; Zeus Publications: Mermaid Waters, Australia, 2015.
44. Tjhung, E.; Nardini, C.; Cates, M.E. Cluster Phases and Bubbly Phase Separation in Active Fluids: Reversal of the Ostwald Process. *Phys. Rev. X* **2018**, *8*, 031080. [[CrossRef](#)]
45. Yamanaka, K.; Takagi, Y.; Inoue, T. Reaction-Induced Phase Separation in Rubber-Modified Epoxy Resins. *Polymer* **1989**, *30*, 1839–1844. [[CrossRef](#)]
46. Wang, W.; Liu, Q.-X.; Jin, Z. Spatiotemporal Complexity of a Ratio-Dependent Predator–Prey System. *Phys. Rev. E* **2007**, *75*, 051913. [[CrossRef](#)] [[PubMed](#)]
47. Das, P.; Jaiswal, P.K.; Puri, S. Surface-Directed Spinodal Decomposition on Chemically Patterned Substrates. *Phys. Rev. E* **2020**, *102*, 012803. [[CrossRef](#)] [[PubMed](#)]
48. Posada, E.; López-Salas, N.; Carriazo, D.; Muñoz-Márquez, M.A.; Ania, C.O.; Jiménez-Riobóo, R.J.; Gutiérrez, M.C.; Ferrer, M.L.; del Monte, F. Predicting the Suitability of Aqueous Solutions of Deep Eutectic Solvents for Preparation of Co-Continuous Porous Carbons via Spinodal Decomposition Processes. *Carbon* **2017**, *123*, 536–547. [[CrossRef](#)]
49. Stenhammar, J.; Tiribocchi, A.; Allen, R.J.; Marenduzzo, D.; Cates, M.E. Continuum Theory of Phase Separation Kinetics for Active Brownian Particles. *Phys. Rev. Lett.* **2013**, *111*, 145702. [[CrossRef](#)]
50. Stenhammar, J.; Marenduzzo, D.; Allen, R.J.; Cates, M.E. Phase Behaviour of Active Brownian Particles: The Role of Dimensionality. *Soft Matter* **2014**, *10*, 1489–1499. [[CrossRef](#)]
51. Cates, M.E.; Tailleur, J. Motility-Induced Phase Separation. *Annu. Rev. Cond. Matter Phys.* **2015**, *6*, 219–244. [[CrossRef](#)]